Islamic University Journal of Applied Sciences (IUJAS)

https://journals.iu.edu.sa/jesc

Volume VII, Issue I, 1 July 2025, Pages 209-226

Power Optimization in MIMO-NOMA VLC Systems Using Fractional and Dynamic Frequency Reuse

Nesrine Titi, Sofiane Haddad *, Ammar Soukkou

Department of Electronics, Faculty of Sciences and Technology, MSB Jijel University, Algeria

*Corresponding author: (S. Haddad), *Email Address* s_haddad@univ-jijel.dz

Abstract

This paper investigates power allocation strategies for enhancing the achievable sum rate in indoor Multi-User Visible Light Communication (MUVLC) systems using Multiple-Input Multiple-Output Non-Orthogonal Multiple Access (MIMO-NOMA). Two frequency reuse methods—Fractional Frequency Reuse (FFR) and Dynamic Frequency Reuse (DFR)—are proposed and evaluated against the existing Normalized Gain Difference Power Allocation (NGDPA) technique. Simulation results for a (2×2) MIMO-NOMA-VLC system show that while FFR can offer substantial performance improvements under favorable conditions, its effectiveness diminishes and may even underperform in specific scenarios. In contrast, DFR consistently outperforms NGDPA across a range of network conditions, demonstrating robust and reliable sum rate enhancement. This consistent adaptability makes DFR a more effective and preferred solution for optimizing power allocation and maximizing spectral efficiency in indoor VLC environments.

Keywords: Multiple-input, Multiple-output, Non-orthogonal multiple access, Visible light communication systems, Power allocation methods, Fractional Frequency Reuse, Dynamic Frequency Reuse.

---

https://doi.org/10.63070/jesc.2025.013
Received 05 April 2025; Revised 10 May 2025; Accepted 23 May 2025.
Available online 28 May 2025.
Published by Islamic University of Madinah on behalf of *Islamic University Journal of Applied Sciences*.

1. Introduction

VLC has gained significant attention as an emerging technology for advancing 5G and B5G (beyond 5G) wireless systems. One of the key advantages of VLC is that it operates in a wide license-free spectrum, which makes it an attractive option for wireless communication. The use of VLC technology allows for the exploitation of the visible light spectrum, which is typically not used for communication purposes, thus offering a vast and unutilized resource for wireless data transmission. Moreover, VLC can potentially offer high-speed data transmission, low latency, and high security, making it a strong contender for the upcoming generation of wireless networks.

In the last years, there has been a growing focus on optimizing the allocation of transmit power values to users in combined NOMA-VLC networks. This involves determining the appropriate power values to be assigned to each user by the LED transmitter. NOMA is a technique designed to enable several users to be served using the same resource. VLC systems, on the other hand, offer the advantage of a channel condition that typically stays consistent and only changes with the movement of users. Thus, VLC can be a particularly effective approach for enhancing the effectiveness of NOMA-based systems. By leveraging the stability of the VLC channel, it becomes possible to optimize the transmit power values assigned to each user in the NOMA-VLC network, thereby improving the overall system performance. In [1], a power allocation method named NLGRPA (Normalized Logarithmic Gain Ratio Power Allocation) has been suggested for NOMA-assisted MIMO-VLC networks. This method efficiently allocates power by utilizing optical channel information from all LEDs on the transmitter. The authors have indicated that the suggested NLGRPA method has achieved a substantial enhancement in terms of the achievable sum rate compared to conventional power allocation approaches. In [2], a 2-user 2×2 MIMO-NOMA-VLC system using OOK (On-Off Keying) and L-PPM (L-pulse position modulation) is proposed, and the authors derived the BER (Bit Error Rate) formulas for the system. The authors observed that increasing the number of photo-detectors at the receiver fails to substantially enhance the system's error performance. To enhance the error performance of the OOK and L-PPM modulated MIMO-NOMA-VLC system, two dynamic field of view (FOV) strategies are proposed. These strategies outperform the existing fixed FOV receivers in a MIMO environment.

Moreover, [3] provides a thorough overview of user pairing and power allocation techniques for NOMA-based VLC systems. The authors have discussed various user pairing schemes and power allocation strategies, highlighting that high channel gain difference is a significant concern when implementing

NOMA effectively. In [4], a secure NOMA VLC system with OFDM modulation is proposed and experimentally demonstrated. In which chaotic phase rotations in the selected mapping has been used to decrease the PAPR ratio (Peak-to-Average Power Ratio) of the transmitted OFDM-NOMA signal. The proposed scheme provides two-fold protection against eavesdroppers with a large key space and guarantees the privacy between legitimate users while minimizing the PAPR. Besides, in [5], NOMA has been combined with VLC to create a high-speed and error-free network. The authors have used OOK and L-PPM in a 2-user downlink NOMA VLC-based system, and evaluated the system's performance with perfect and imperfect channel state information (CSI). As findings, giving at least 60% of the power to the far user resulted in significantly better performance for that user, and L-PPM modulation with $L > 2$ has outperformed OOK modulation. Additionally, increasing the order of modulation has improved the performance for both users. However, if the far user shifts away from the fixed location of the near user and toward the corner of the room, their error performance suffers. The performance of both users also has been improved with a smaller FOV, with the close user performing better with a FOV of less than 35° than the far user with a FOV of 60°. Both OOK and L-PPM modulated NOMA-VLC systems have performed poorly with channel estimation error, and this effect is worsened with more complex modulation techniques. In [6], a NOMA VLC network that can serve 2, 3, or 4 clients simultaneously using NHS-OFDM IFFT/FFT size efficient (SE) OFDM format has been proposed and developed. The authors conducted a numerical analysis of the impact of signal amplitude on bit error rate (BER) performance for various users, and compared the suggested system with a common HS OFDM modulation example, termed DCO-OFDM NOMA-VLC system.

Furthermore, the authors in [7] have employed NOMA in VLC systems and proposed a simplified gain ratio power allocation method (S-GRPA) as a low-complexity power allocation method for indoor NOMA-based VLC systems. The authors found that the suggested S-GRPA system used a look-up table to obtain channel gains, and although users with stronger channel quality experienced some performance variations during a single trial, the average data rate over multiple trials was higher than that achieved using the conventional GRPA method. Besides, the suggested S-GRPA system has minimal feedback overhead and computational complexity, suggesting a promising future for high-speed VLC systems. An effective framework for a combined power line communication (PLC) and VLC system has been explored in [8], with a focus on its potential applications in smart grids. The work has explored NOMA as a means of growing the capacity of the integrated system, given the opportunistic features of both the VLC and PLC systems, which focus primarily on lighting and power delivery. The paper [9] provided a comprehensive review of previous studies on 5G and B5G, and compared them to various paper's contributions, distinctiveness, and advantages. It covered various topics, including the prerequisites and technologies for 5G and B5G, channel analysis, and NOMA's significance in these networks, different types of NOMA, the architecture of the NOMA network, mobility management (MM), asynchronous and synchronous operations in NOMA, energy and green aspects of NOMA in 5G and B5G, challenges faced by NOMA, solutions for these challenges, and NOMA's performance indicators. Also, in [10] the authors have demonstrated the feasibility of using NOMA in optical MIMO-VLC systems. They showed that the NOMA scheme provided a good trade-off balancing throughput and fairness, and increased system capacity for a higher number of users. The authors proposed utilizing channel estimation techniques, specifically ISFA and MMSE, to remove inter-user interference, along with effective channel equalization for MIMO demultiplexing.

Challenges and limitations of integrating NOMA with 5G and future wireless technologies were highlighted in [11], including signaling, practical implementation, resource allocation, and security issues. Various analytical, matching theory, game theory, graph theory, and machine learning approaches have been proposed to address these challenges. The authors have conducted an in-depth investigation and comparison of different options, and provided insights into the operability and usability of NOMA for qualitative study. They also suggested intriguing research paths and challenges for applying PD NOMA to current and next-generation wireless networks. In [12], the authors have recommended a framework for user connection and power distribution in a 2-tier heterogeneous network using non-orthogonal multiple access. They took into consideration channel uncertainties and real-world wireless communication environments by presenting them as probability constraints. The non-convex objective function that regulated intra-cell and inter-cell interference was solved using the logarithmic approximation approach, and a method for dispersed user association was developed based on Lagrangian dual analysis. The authors concluded that their proposed approach outperformed both the FTPA algorithm and the conventional OMA algorithm in a dynamic communication environment. Further, in [13] the authors have presented a literature survey that highlights the need to shift from the current RF band to VLC due to its limitations. They have proposed a mathematical model that considers reflection from various reflectors and suggest approaches such as Bragg grating, adaptive beam shifting, and hybrid access technology to enhance signal strength.

An investigation of a unique problem of blind source separation in communication systems using observed magnitude-only measurements of its convolutive mixing has been presented in [14]. In which a blind receiver architecture that is capable of reconstructing signals from their recorded phaseless convolutive mixture with the trade-off of requiring more measurements has been introduced. Both deterministic and stochastic subspaces can be used with the given strategy, and the experimental results and theoretical findings are in agreement. In [15], scientists have reviewed current publications on 6G, covering its introduction, core technologies, basic architecture, challenges, and relevant factors. The study included several applications and architectural descriptions, clarifying the current state-of-the-art and the direction of future research. Moreover, in [16], the authors have presented a comprehensive perspective on a number of OWC enabling technologies and survey probable OWC system problems. They have studied FSO and VLC as prospective OWC system implementation strategies and examined potential characteristics and categorizations of OWC systems, critical allowing technologies, connection design specifications and modulation techniques, main impairments and strategies to address them, and security concerns and methods to secure OWC. The work in [17], explored the use of multi-level AM modulation combined with trellis coding in a NOMA's downlink channel for VLC. The authors used a trellis decoder to implement non-orthogonal transmission through successive interference cancellation and superposition coding. They have compared two maximum likelihood signal detection levels for related 4 and 8 trellis-coded modulations. In [18], the authors discussed the application of NOMA technique to increase the attainable sum rate of MIMO-based multi-user VLC systems. They have proposed an NGDPA method to guarantee efficient and low-complexity power allocation in indoor MIMO-NOMA-based VLC systems. Through numerical simulations, they have demonstrated that NOMA with NGDPA attains a significantly higher sum rate than NOMA with GRPA in an indoor 2×2 MIMO-VLC system. They also found that applying NOMA with NGDPA in the 2×2 MIMO-VLC system with 3-users can boost the sum rate by up to 29.1%. The authors have suggested that MIMO-NOMA using the suggested NGDPA approach is potential for next high-speed multi-user VLC systems.

Furthermore, a broad-based multi-user MIMO-NOMA-VLC framework that uses OOK modulation and M×N LOS links for each user, to create a resilient, high-performance, and error-free network designed for multi-user environments, has been proposed in [19]. The authors have developed a closed form expression to calculate the error probability for the suggested system, taking into account a real-world example of imperfect SIC. Also, a thorough analysis of a 2×2 MIMO-NOMA-VLC system with three users, generating a precise closed-form formula of the system's error probability from this analysis has been presented. In [20], a HPD-LACO-OFDM (Hierarchical Pre-Distorted Layered Asymmetrically Clipped Optical) system for NOMA, providing excellent optical power efficiency and spectrum efficiency has been developed. The experiment showed that the three layers HPD-LACO-OFDM based NOMA-VLC network outperformed the DCO-OFDM based NOMA-VLC network in terms of BER while requiring just half as much DC power. In [21], the authors have analyzed the performance of short-packet communication (SPC) within a downlink NOMA-VLC system. The SPC-NOMA VLC system was found to offer greater reliability and lower latency compared to LPC-NOMA VLC systems. Besides, the SPC-NOMA-VLC system outperformed the SPC-OMA VLC system in terms of throughput, latency, and dependability. In [22], researchers have proposed a NOMA-OFDM-VLC system based on non-Hermitian symmetry (NHS) inverse-fast Fourier-transform (IFFT)/FFT size efficient (SE), which was experimentally tested. The proposed strategy outperformed the HS based on DCO-OFDM NOMA-VLC system. A demodulator for NOMA-VLC based on convolutional neural networks (CNNs), which simultaneously performed signal recovery and compensation has been proposed in [23]. The proposed CNN-based receiver effectively corrects both linear and nonlinear distortions caused by multipath dispersion, limited modulation bandwidth, and LED nonlinearity, outperforming SIC and JD-based receivers. In [24], a development of a joint PLC-VLC power allocation (JPA) technique to maximize the sum throughput, which was found to outperform the SPA and NGDPA benchmarks under various minimum rate requirements and user densities has been presented. However, in the proposed PLC-VLC network, several problems related to multiple users power allocation and subcarrier allocation still need to be addressed.

Additionally, in [25], researchers proposed an OQAM/OFDM-NOMA modulation strategy, combining offset QAM/OFDM and non-orthogonal access, applicable to a multi-user, non-synchronized multi-cell VLC system. The optimal power ratio between the cell-center user and the cell-edge user was investigated, and the OQAM/OFDM-NOMA was found to be promising to increase user connectivity, stronger reliability, and enhanced user fairness for the multi-cell VLC system. Also, in [26], the authors conducted a theoretical analysis of errors in a downlink power-domain NOMA-based VLC system utilizing higher-order modulation schemes, considering the potential impact of imperfect SIC. The SER in NOMA-based systems was found to decrease when an appropriate PA was selected based on the users' modulation orders. In [27], the use of NOMA in VLC networks is investigated to enhance the sum rate performance and overcome the limitations of narrow modulation bandwidth. The authors have focused on power control for indoor downlink NOMA-VLC systems with a single LED and multiple users, and they found that the MFOPA scheme performed better in terms of sum rate and user fairness compared to existing SPA and GRPA schemes. Moreover, in [28], the authors have examined a downlink multiuser VLC network with fluctuating vertical orientation and location of users, and they found that NOMA transmission with practical feedback methods generated optimal sum-rate performance. The authors in [29], have proposed a hybrid VLC-RF system using NOMA technology with imperfect channel-state information, and they found that the performance of both NOMA and OFDMA systems is affected by the quantity of CSI error, but the hybrid VLC-RF system with NOMA outperformed the VLC-Only System with NOMA in imperfect CSI scenarios. These findings are useful for the development of hybrid VLC-RF systems.

Recently, several techniques based on frequency reuse are proposed to optimize communication system's performance. Among these techniques are fractional frequency reuse (FFR) and dynamic frequency reuse (DFR) schemes. Both FFR and DFR work by dividing the entire bandwidth into multiple sub-bands, which are strategically allocated within the system to optimize power distribution. The authors in [30] have introduced a generalized FFR model for Ultra Dense Networks (UDNs), enabling better performance without increasing Base Station (BS) power usage. It addressed challenges in frequency band reuse caused by ultra-high BS densities, providing analytical solutions for user coverage probabilities. The work in [31] discussed FFR to manage interference in cellular networks, employing dynamic thresholding techniques like Otsu's and entropy methods. Furthermore, [32] introduced an approach to assess the uplink cellular spectral efficiency of MC-CDMA systems with fractional and soft frequency reuse. In [33], the authors proposed a coordination scheme for D2D communications, leveraging LTE's FFR to reuse uplink spectrum. Their approach adjusts transmissions to minimize interference with cellular uplinks, ensuring effective peer discovery while conserving radio resources. Evaluation demonstrates minimal impact on cellular transmissions and sufficient D2D discovery. Also, in [34], DFR and Weighted-DFR algorithms have been proposed to address inter-cell interference in indoor optical attocell networks utilizing LEDs for visible light communication. Also, the study in [35] explored the use of NOMA techniques MUVLC systems with MIMO technology. A power allocation technique based on the Water-Filling Algorithm is proposed and compared to NGDPA. Simulation results for a 2x2 indoor MIMO-NOMA-VLC system showed that the Water-Filling technique outperforms NGDPA, achieving a 3% higher sum rate gain at higher offsets.

In this work, we propose two methods to optimize power allocation in MIMO-NOMA VLC systems utilizing frequency reuse schemes. The rest of the paper is structured as follows: Section 2 details the system model of the indoor VLC network, including its characteristics and problem formulation. Section

3 introduces power allocation techniques and the developed models related to FFR and DFR. Section 4 presents the simulation results. Finally, Section 5 provides the conclusions.

2. System Model

This section presents a mathematical model for a 2x2 indoor MIMO-NOMA-VLC system, where each user has two photodiodes for enhanced signal reception and utilizes the full LED modulation bandwidth (**Figure** 1). The system uses DCO-OFDM modulation for high spectral efficiency and interference resilience, with potential for extension to more complex setups.

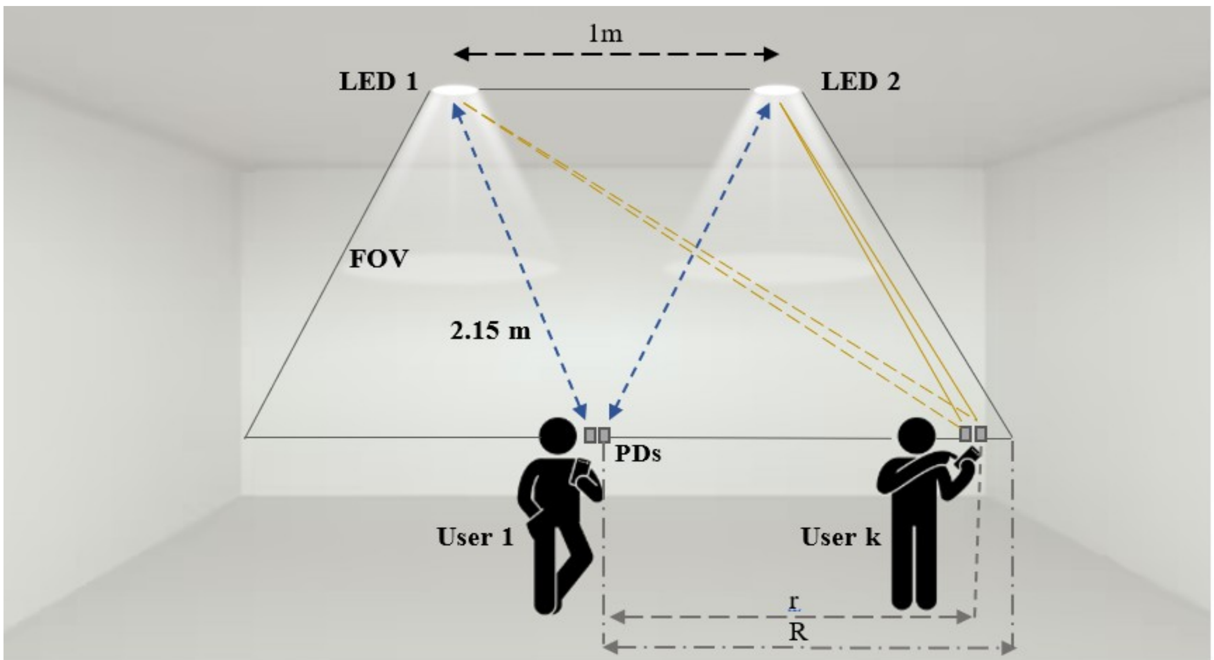

Figure 1. Graphic of a 2x2 MIMO-NOMA-VLC system.

Figure 2 illustrates the 2x2 MIMO-NOMA-VLC system using DCO-OFDM modulation. Input signals $x_1(t)$ and $x_2(t)$ are applied to LEDs 1 and 2, respectively. After DCO-OFDM modulation and DC polarization, the input signal $x_i(t)$ for the i-th LED is represented as [18]:

$$x_i(t) = \sum_{k=1}^{K} \sqrt{\rho_{i,k}} s_{i,k}(t) + I_{\mathrm{DC}} \quad (1)$$

The signal $s_{i,k}(t)$ is the signal for the k-th user from the i-th LED, with $\rho_{i,k}$ being the electrical power allocated to the k-th user by the i-th LED, and I_{DC} representing the DC bias for each LED to ensure the signal $x_i(t)$ remains non-negative, as required for intensity modulation in VLC systems. $s_{i,k}(t)$ Encodes user data and is orthogonal to other subcarriers to minimize interference. Upon modulation, the signal is emitted by the LED and captured by the users' photodiodes. The reception process utilizes MIMO-NOMA to separate signals from various LEDs, followed by demodulation to retrieve the original data, with further details provided below.

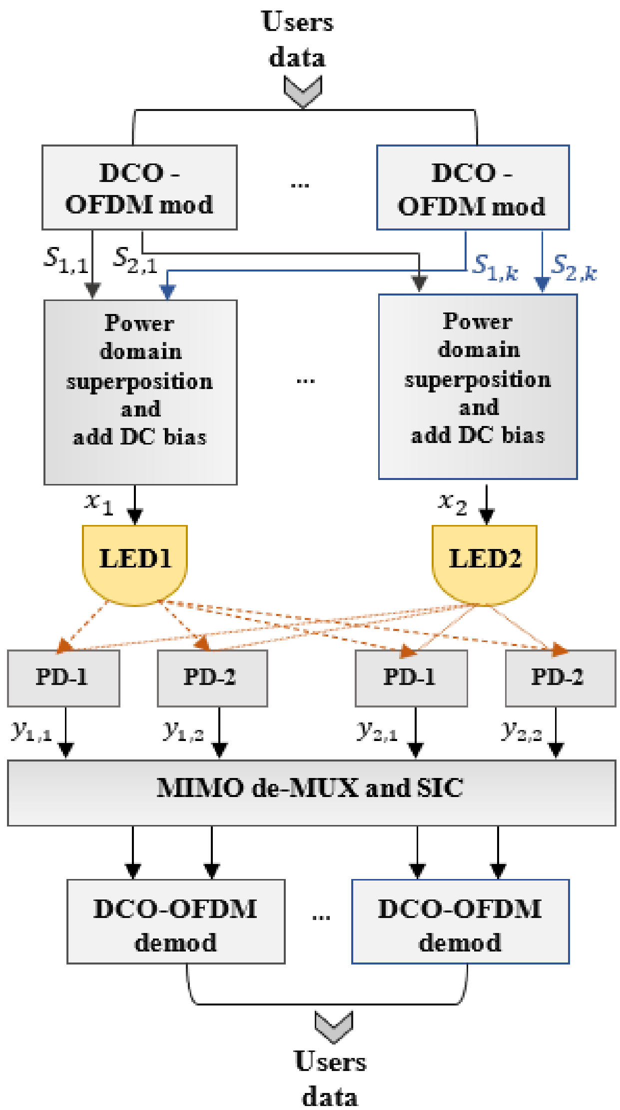

Figure 2. Functional diagram of a VLC system using DCO-OFDM modulation, based on 2x2 MIMO-NOMA [18].

To maintain consistent electrical power (P_{elec}) per LED, the following power constraint is applied:

$$\sum_{k=1}^{K} \rho_{i,k} = P_{\text{elec}} \quad (2)$$

For simplicity, P_{elec} per LED is set to 1. The received electrical signal by the k-th user after transmission is represented by the following vector:

$$\mathbf{y}_k = \gamma P_{opt} \zeta \mathbf{H}_k \mathbf{x} + \mathbf{n}_k \quad (3)$$

The received signal by the k-th user considering the responsivity γ of the photodetector and the LED optical output P_{opt} is characterized by a modulation index ζ, a channel matrix $H_K(2x2)$, and an electrical signal vector $x = [x1\ x2]^T$. The additive noise is denoted by the vector n_k.

This paper, as in [18], considers the Lambertian radiation pattern for each LED, focusing solely on LOS component. The LOS optical channel gain between the i-th LED $(i = 1, 2)$ and the j-th user $(j = 1, 2)$ is then calculated as follows:

$$h_{ji,k} = \frac{(m+1)A_{PD}}{2\pi d^2} \mu\eta \cos^m(\varphi) \cos(\theta) \quad (4)$$

The LOS optical channel gain from the i-th LED to the j-th user depends on factors like the LED's half-power angle, Lambertian order m, A_{PD} active area, optical filters, lenses, LED-user distance, emission angle φ, and incidence angle θ. If the incident light is outside the receiver's FOV, the gain is zero. MIMO demultiplexing and a low-complexity zero-forcing (ZF) method are used for data recovery. After demultiplexing and power normalization, the electrical signal vector for the j-th user is represented by the following formula:

$$\tilde{\mathbf{x}}_k = \mathbf{x} + \frac{1}{\gamma P_{opt} \xi} \mathbf{H}_k^{-1} \mathbf{n}_k \quad (5)$$

The MIMO-NOMA-VLC system uses multiple LEDs and DCO-OFDM modulation. The input signal $x_i(t)$ for the i-th LED is derived from DCO-OFDM modulation, power superposition in the frequency domain, and addition of DC bias. The signal $s_{i,k}(t)$, meant for the k-th user from the i-th LED, has electrical power $\rho_{i,k}$ and DC bias I_{DC}. To maintain constant total electrical power $Pelec$ for each LED, a power constraint is applied. After free-space propagation, the received electrical signal vector at user k is $\boldsymbol{H}_k[x1\ x2]^T + \boldsymbol{n}_k$, where γ is the responsivity, P_{opt} is the optical output of the LED, ζ is the modulation index, $\boldsymbol{H_k}$ is the 2x2 channel matrix of user k, and $\boldsymbol{n_k}$ is the additive noise vector. Optical channel gains are calculated using the Lambertian radiation pattern and direct visibility component. Decoding uses MIMO demultiplexing with ZF and basic channel inversion. User decoding order for each LED is based on the optical channel gains' sum for every user, sorted in descending order. SIC decoding is performed for every LED and user using the inverse of the channel matrix $\boldsymbol{H_k}$.

$$h_{1i,1} + h_{2i,1} > h_{1i,2} + h_{2i,2} > \cdots > h_{1i,K} + h_{2i,K} \quad (6)$$

The order of the decoding for the i-th LED is then established as follows:

$$O_{i,1} < O_{i,2} < \cdots < O_{i,K}. \quad (7)$$

This study assumes perfect SIC without error propagation in the signal, and the two users' data is gotten through DCO-OFDM demodulation.

3. Power allocation methods

3.1. Power Allocation with Normalized Gain Difference (NGDPA)

The NGDPA method optimizes power allocation in MIMO-NOMA VLC systems by efficiently distributing emission power among users sharing the same resource. It calculates the normalized gain difference by estimating transmitter-receiver channels, computing the gain difference between user pairs with mutual interference considered, and dividing this difference by the total sum of gains. Power is then allocated to maximize the normalized gain difference, with users having better channels receiving less power. The allocation for users k and k+1 on the i-th LED is based on the optical channel gain difference [18].

$$\rho_{i,k} = \left(\frac{h_{1i,1}+h_{2i,1}-h_{1i,k+1}-h_{2i,k+1}}{h_{1i,1}+h_{2i,1}}\right)^{k} \rho_{i,k+1} \quad (8)$$

3.2. Power Allocation using Fractional Frequency Reuse

FFR enhances spectral efficiency in MIMO-NOMA-VLC systems by dividing the frequency spectrum into fractions and allocating them to different users or cells. The power allocation scheme based on FFR is modeled as follows:

$$\Delta h_{i,k}^{FFR} = \alpha.\Delta h_{i,k} \quad (9)$$

Where $\Delta h_{i,k}^{FFR}$ is the modified optical channel gain difference incorporating FFR for user k in the i-th LED, $\Delta h_{i,k}$ is the original optical channel gain difference for user k in the i-th LED, and α represents the FFR factor (α equal to 0.5 in our case study). Using the modified optical channel gain differences, the power allocation for the k-th user in the i-th LED incorporating FFR becomes:

$$\rho_{i,k}^{FFR} = \left(\frac{\Delta h_{i,k}^{FFR}}{h_{1i,k1} + h_{2i,1}} \right)^{k} \rho_{i,k+1} \tag{10}$$

In this equation, we use $\Delta h_{i,k}^{FFR}$ to reflect the impact of FFR on the optical channel gain differences. This adjusted power allocation considers the modified channel conditions due to FFR while maintaining the same power allocation relationship between consecutive users within the LED.

3.3. Power Allocation with Dynamic Frequency Reuse

DFR is an algorithm for power allocation in MIMO-NOMA-VLC systems, where multiple users share the same transmission resource. DFR dynamically allocates frequency resources based on traffic and channel conditions. The DFR factor, denoted as β, represents the dynamic allocation factor for optical channel gain differences, which are then modified accordingly.

$$\Delta h_{i,k}^{DFR} = \beta_k . \Delta h_{i,k} \tag{11}$$

Where $\Delta h_{i,k}^{DFR}$is the modified optical channel gain difference incorporating DFR for the k-th user in the i-th LED, $\Delta h_{i,k}$ is the original optical channel gain difference for the k-th in the i- th LED and $\beta_k$is the DFR factor for the k-th user. The DFR factor is the ratio of power allocated to each LED based on channel gains. Power allocation for user k on the i-th LED incorporating DFR is then:

$$\rho_{i,k}^{DFR} = \left(\frac{\Delta h_{i,k}^{DFR}}{h_{1i,1} + h_{2i,1}} \right)^{k} \rho_{i,k+1} \tag{12}$$

The term $\Delta h_{i,k}^{DFR}$ is used to reflect the impact of DFR on the optical channel gain differences. This adjusted power allocation incorporates dynamic frequency allocation based on channel conditions and traffic demands while preserving the power allocation relationship between consecutive users within the LED. Including DFR enhances the adaptability and efficiency of the MIMO-NOMA-VLC system, especially under varying traffic loads and channel conditions.

4. Results and Discussion

4.1. System configuration

We evaluate a 2×2 MIMO-NOMA-VLC system using various power allocation techniques through simulations, based on the configuration in [18]. The system features LEDs spaced 1 meter apart and 2.15 meters vertically from users. Each LED has a 10 W output power with a 60° beam angle, a 10 MHz modulation bandwidth, and a 0.5 modulation index. Detectors have a 1 cm² active area, a 0.53 A/W responsivity, and are spaced 4 cm apart. Optical filter and lens gains are 0.9 and 2.5, respectively (see Table 1). We assess performance with a fixed user 1 at the center between LEDs 1 and 2, 2 meters from the coverage edge. Other users, denoted as K, are uniformly distributed with distances defined by r/R, where R is the distance from user 1 to the edge of the coverage. Furthermore, the normalized offset of user k regarding user 1 is calculated as $\frac{(k-1)r}{(K-1)R}$, which determines the position of each user relative to user 1, Table 2.

Table 1. System configuration.

Parameter	Value
LED Spacing	1 m
Vertical Distance (LEDs-Users)	2.15 m
LED Output Power	10 W
LED Beam Angle (half-power)	60°
Modulation Bandwidth	10 MHz
Modulation Index	0.5
Photodetector Area	1 cm²
Photodetector Responsivity	0.53 A/W
Detector Spacing (per User)	4 cm
Optical Filter Gain	0.9
Optical Lens Gain	2.5

Table 2. User's description for performance evaluation.

Parameter	Description
User 1	Fixed user, center between LEDs 1 & 2, 2 m from system edge.
Users K	K users uniformly distributed around User 1 at distance r.
Normalized Offset $(\boldsymbol{r/R})$	Relative distance of User k to User 1 (R = distance between User 1 and system edge).
Normalized Offset $\left(\frac{(\boldsymbol{k-1})\boldsymbol{r}}{(\boldsymbol{K-1})\boldsymbol{R}}\right)$	User k position relative to User 1 (k = user number).

4.2.Comparison of achievable sum rates for different power allocation techniques

Based on **Figure** 3 and the numerical results presented in Table 3, the achievable sum rate varies with the normalized offset (r/R) for the power allocation methods. The NGDPA method shows a decreasing sum rate with increasing offset due to higher interference. FFR has a sharper decline in sum rate as the offset increases, especially in the LED1+LED2 scenario, indicating higher sensitivity to offset changes. DFR maintains the highest sum rates among the methods but also shows a rapid decline with increasing offset. Overall, while NGDPA offers stable performance, DFR provides the highest sum rates but is more sensitive to offset variations, outperforming both NGDPA and FFR. **Figure** 3 shows the mean performance of NGDPA, FFR, and DFR across different normalized offsets, with bars representing LED1+LED2, LED1, and LED2 configurations. Error bars indicate standard deviation, reflecting performance variability. Statistical comparisons reveal that DFR significantly outperforms NGDPA and FFR, with p-values of 0.0010071 (NGDPA vs. FFR), 9.2691×10^{-9} (NGDPA vs. DFR), and 5.6372×10^{-7} (FFR vs. DFR), confirming the superior performance of DFR over both NGDPA and FFR. **Figure** 4 and **Figure** 5 compare the Average Bit Error Rate (ABER) and Average Signal to Noise Ratio (ASNR) for various methods using 4-QAM modulation. NGDPA consistently provides the best ASNR across all offsets but shows significant ABER beyond an offset of 0.5. FFR maintains low ABER up to an offset of 0.5 but experiences a progressive decline in ASNR. DFR also has low ABER up to 0.5 but follows with a decrease in ASNR. NGDPA is ideal for applications prioritizing high signal quality, while FFR and DFR are better for maintaining low error rates at moderate offsets.

Table 3. Comparison of NGDPA, FFR, and DFR methods (Sum rate Mbits/s vs. Normalized Offset r/R).

Normalized Offset r/R	Sum rate Mbits/s								
	NGDPA method			**FFR method**			**DFR method**		
	LED1+ LED2	LED1	LED2	LED1+ LED2	LED1	LED2	LED1+ LED2	LED1	LED2
0.1	113.6799	56.4781	57.2018	151.7281	75.2768	76.4513	279.2620	138.5732	140.6888
0.2	113.4502	56.5029	56.9473	150.2587	73.9810	76.2777	276.2659	136.3171	139.9487
0.3	112.1914	56.5035	55.6878	147.8315	72.2551	75.5763	271.2661	133.4380	137.8281
0.4	110.1434	56.4908	53.6526	144.4697	70.1275	74.3422	264.2201	129.9806	134.2394
0.5	106.3947	56.4595	49.9352	140.1866	67.6138	72.5727	255.0162	125.9234	129.0927
0.6	111.8666	56.3902	55.4764	134.9635	64.7073	70.2563	243.4436	121.1567	122.2869
0.7	112.1559	56.2273	55.9286	128.7119	61.3604	67.3514	229.1520	115.4680	113.6840
0.8	111.6286	55.8034	55.8252	121.1891	57.4470	63.7421	211.5407	108.4984	103.0423
0.9	109.8027	54.6114	55.1914	111.7640	52.6538	59.1103	189.3764	99.5615	89.8150

1	104.4413	51.8753	52.5659	98.4930	46.1082	52.3848	159.5254	86.9561	72.5693

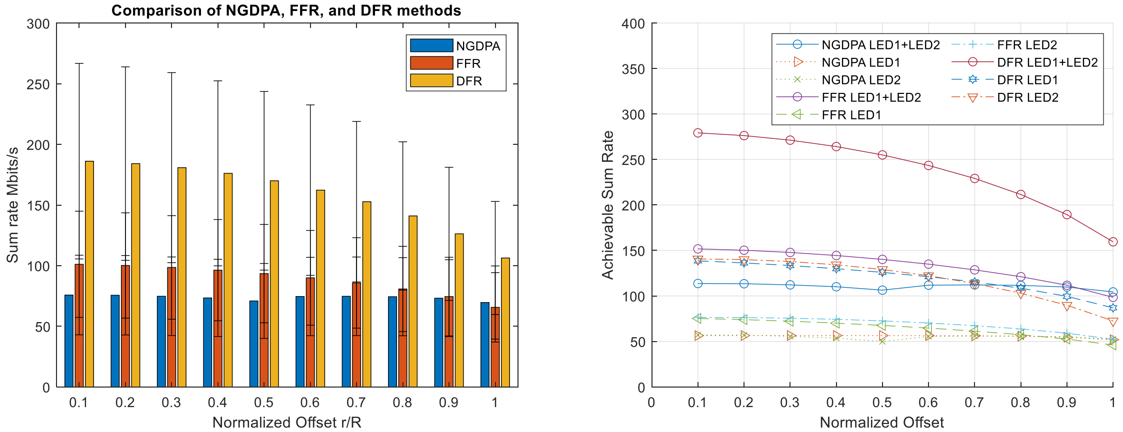

Figure 3. Achievable sum rate vs. normalized offset using NGDPA, FFR, and DFR techniques for NOMA-VLC system.

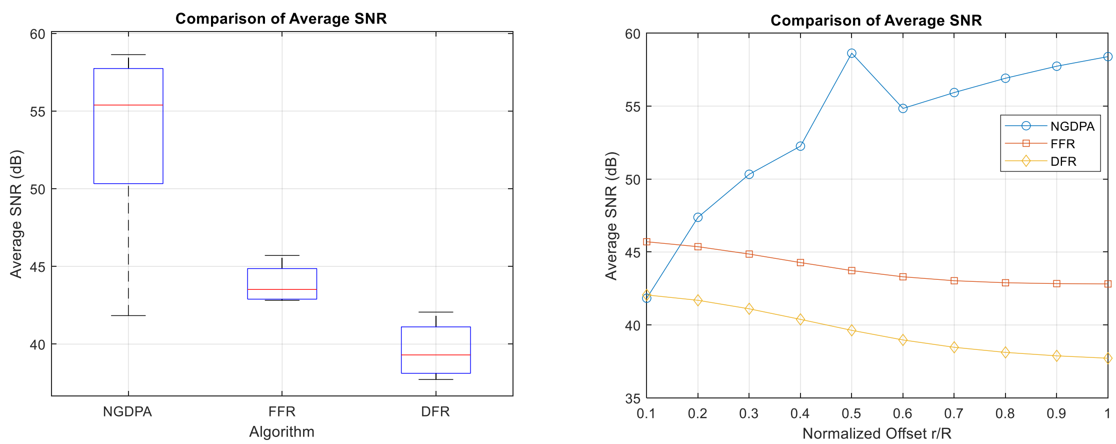

Figure 4. Average SNR using NGDPA, FFR, and DFR techniques for NOMA-VLC system.

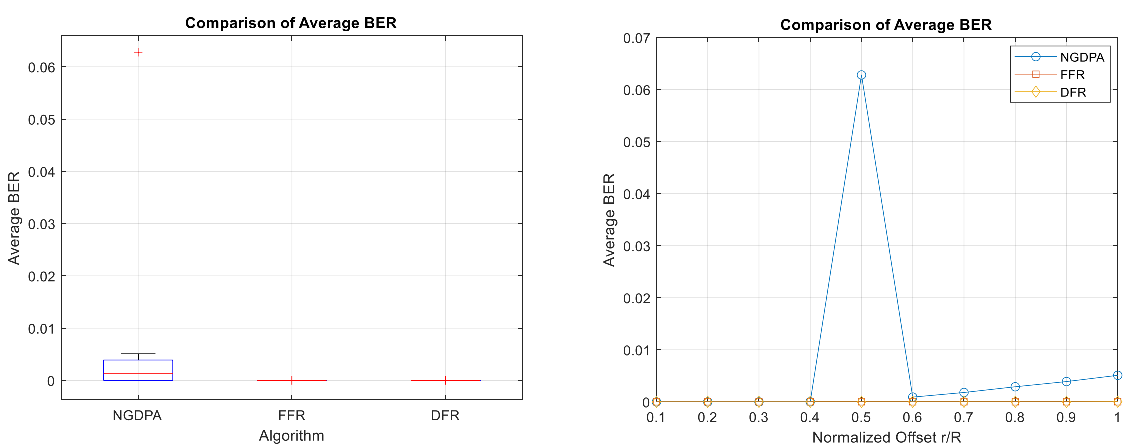

Figure 5. Average BER using NGDPA, FFR, and DFR techniques for NOMA-VLC system.

Figure 6 shows that both FFR and DFR outperform NGDPA, though their gains vary. FFR starts with a gain of over 30% but decreases and becomes negative (around -5%) as the normalized offset (r/R) increases, indicating worse performance than NGDPA under certain conditions. In contrast, DFR consistently offers a higher gain in sum rate compared to NGDPA across all offsets, with only a slight reduction in gain as conditions change. This suggests that DFR is more effective in optimizing sum rate, making it the preferred method for most network scenarios.

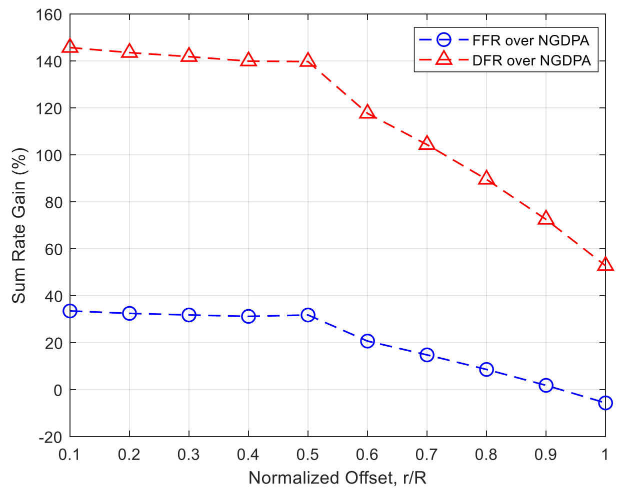

Figure 6. Percentage Gain of sum rate based FFR & DFR techniques over NGDPA method.

5. Conclusion

In this paper, we have studied the multi-user system based on MIMO-NOMA in VLC. We analyzed the performance of three different power allocation methods, including the NGDPA method, the FFR method, and the DFR method. Results have shown that these power allocation methods can improve system performance. The DFR algorithm demonstrated the highest achievable sum rate, followed by the FFR method and the NGDPA method. FFR optimally allocates frequency resources by dividing the cell into multiple zones with different reuse factors, there by effectively reducing interference and enhancing spectral efficiency. Meanwhile, DFR dynamically adjusts frequency allocation based on the traffic load, allowing for more flexible and efficient spectrum utilization. In contrast, the NGDPA method, while theoretically promising, falls short in practical implementation due to its limited adaptability to dynamic network conditions and its inability to effectively mitigate interference. The choice of power allocation method in MIMO-NOMA-VLC systems depends on the specific application requirements, with key considerations including computational complexity, accuracy, and overall system performance. Techniques such as Fractional Frequency Reuse (FFR) and Dynamic Frequency Reuse (DFR) can enhance spectral efficiency and adaptability, though FFR may suffer from rigidity while DFR can introduce significant computational overhead. These trade-offs underscore the need for adaptive or hybrid approaches tailored to deployment scenarios. This work paves the way for future research aimed at further optimizing system performance, including the exploration of machine learning-based dynamic reuse factor adjustment and hybrid FFR/DFR frameworks to meet the real-time demands of advanced communication environments.

Conflict of interest statement:

On behalf of all authors, the corresponding author states that there is no conflict of interest.

Data availability

All data underlying the results are available as part of the article and no additional source data are required.

Author Contributions

All authors contributed to the study and all authors read and approved the final manuscript.

References

[1] H. Wang, F. Wang, and R. Li, "Enhancing power allocation efficiency of NOMA aided-MIMO downlink VLC networks," Opt. Commun. **454**, 124497 (2020).
[2] V. Dixit and A. Kumar, "BER analysis of dynamic FOV based MIMO-NOMA-VLC system," AEU-Int. J. Electron. Commun. **142**, 153989 (2021).
[3] T. Dogra and M.R. Bharti, "User pairing and power allocation strategies for downlink NOMA-based VLC systems: An overview," AEU-Int. J. Electron. Commun. **149**, 154184 (2022).
[4] Y. Wu, Y. Hu, Z. Wan, *et al.*, "Joint security enhancement and PAPR mitigation for OFDM-NOMA VLC systems," Opt. Commun. **508**, 127719 (2022).
[5] V. Dixit and A. Kumar, "An exact BER analysis of NOMA-VLC system with imperfect SIC and CSI," AEU-Int. J. Electron. Commun. **138**, 153864 (2021).
[6] A. Adnan, Y. Liu, C.-W. Chow, *et al.*, "Analysis of non-Hermitian symmetry (NHS) IFFT/FFT Size Efficient OFDM for multiple-client Non-Orthogonal Multiple Access (NOMA) visible light communication (VLC) system," Opt. Commun. **472**, 125991 (2020).
[7] Q. Zhao, J. Jiang, Y. Wang, *et al.*, "A low complexity power allocation scheme for NOMA-based indoor VLC systems," Opt. Commun. **463**, 125383 (2020).
[8] A. Naz, S. Baig, and H.M. Asif, "Non Orthogonal Multiple Access (NOMA) for broadband communication in smart grids using VLC and PLC," Optik **188**, 162–171 (2019).
[9] U. Ghafoor, M. Ali, H.Z. Khan, *et al.*, "NOMA and future 5G & B5G wireless networks: A paradigm," J. Netw. Comput. Appl. **204**, 103413 (2022).
[10] B. Lin, Z. Ghassemlooy, X. Tang, *et al.*, "Experimental demonstration of optical MIMO NOMA-VLC with single carrier transmission," Opt. Commun. **402**, 52–55 (2017).
[11] A. Akbar, S. Jangsher, and F.A. Bhatti, "NOMA and 5G emerging technologies: A survey on issues and solution techniques," Comput. Netw. **190**, 107950 (2021).
[12] Z. Liu, G. Hou, Y. Yuan, *et al.*, "Robust resource allocation in two-tier NOMA heterogeneous networks toward 5G," Comput. Netw. **176**, 107299 (2020).
[13] H. Sharma and R.K. Jha, "VLC enabled hybrid wireless network for B5G/6G communications," Wirel. Pers. Commun. **124,** 1741–1771 (2022).
[14] H. Hameed, A. Ahmed, and U.U. Fayyaz, "Single-channel phaseless blind source separation," Telecommun. Syst. **80,** 469–475 (2022).
[15] P. Meena, M.B. Pal, P.K. Jain, *et al.*, "6G communication networks: introduction, vision, challenges, and future directions," Wirel. Pers. Commun. **125**, 1097–1123 (2022).
[16] S.A.H. Mohsan, A. Mazinani, H.B. Sadiq, *et al.*, "A survey of optical wireless technologies: Practical considerations, impairments, security issues and future research directions," Opt. Quantum Electron. **54**, 187 (2022).

[17] D. Astharini, M. Asvial, and D. Gunawan, “Performance of signal detection with trellis code for downlink non-orthogonal multiple access visible light communication,” Photonic Netw. Commun. **43**, 185–192 (2022).
[18] C. Chen, W.-D. Zhong, H. Yang, *et al.*, “On the performance of MIMO-NOMA-based visible light communication systems,” IEEE Photonics Technol. Lett. **30**, 307–310 (2017).
[19] V. Dixit and A. Kumar, “An exact error analysis of multi-user RC/MRC based MIMO-NOMA-VLC system with imperfect SIC,” IEEE Access **9**, 136710–136720 (2021).
[20] H. Li, Z. Huang, Y. Xiao, *et al.*, “A power and spectrum efficient NOMA scheme for VLC network based on hierarchical pre-distorted LACO-OFDM,” IEEE Access **7**, 48565–48571 (2019).
[21] G.N. Tran and S. Kim, “Performance analysis of short packets in NOMA VLC systems,” IEEE Access **10**, 6505–6517 (2022).
[22] A. Adnan, Y. Liu, C.-W. Chow, *et al.*, “Demonstration of non-hermitian symmetry (NHS) IFFT/FFT size efficient OFDM non-orthogonal multiple access (NOMA) for visible light communication,” IEEE Photonics J. **12**, 1–5 (2020).
[23] B. Lin, Q. Lai, Z. Ghassemlooy, *et al.*, “A machine learning based signal demodulator in NOMA-VLC,” J. Light. Technol. **39**, 3081–3087 (2021).
[24] S. Feng, T. Bai, and L. Hanzo, “Joint power allocation for the multi-user NOMA-downlink in a power-line-fed VLC network,” IEEE Trans. Veh. Technol. **68**, 5185–5190 (2019).
[25] J. Shi, J. He, K. Wu, *et al.*, “Enhanced performance of asynchronous multi-cell VLC system using OQAM/OFDM-NOMA,” J. Light. Technol. **37**, 5212–5220 (2019).
[26] E.M. Almohimmah, and M.T. Alresheedi, “Error analysis of NOMA-based VLC systems with higher order modulation schemes,” IEEE Access **8**, 2792–2803 (2019).
[27] Q. Li, T. Shang, T. Tang, *et al.*, “Optimal power allocation scheme based on multi-factor control in indoor NOMA-VLC systems,” IEEE Access **7**, 82878–82887 (2019).
[28] Y. Yapıcı and I. Güvenç, “NOMA for VLC downlink transmission with random receiver orientation,” IEEE Trans. Commun. **67**, 5558–5573 (2019).
[29] A. Al Hammadi, P.C. Sofotasios, S. Muhaidat, *et al.*, “Non-orthogonal multiple access for hybrid VLC-RF networks with imperfect channel state information,” IEEE Trans. Veh. Technol. **70**, 398–411 (2020).
[30] S.C. Lam and X.N. Tran, “Fractional frequency reuse in ultra dense networks,” Phys. Commun. **48**, 101433 (2021).
[31] A. Onim, S. Musyoki, and P. Kihato, “Selection of optimal SINR threshold in fractional frequency reuse by comparing Otsu’s and entropy method,” Heliyon **8**, e11736 (2022).
[32] H.C. Mora, N.O. Garzón, and C. de Almeida, “On the cellular spectral efficiency of MC-CDMA systems with MMSE multiuser detector employing fractional and soft frequency reuse,” AEU-Int. J. Electron. Commun. **84**, 34–45 (2018).
[33] D. Tsolkas, N. Passas, and L. Merakos, “Enabling device discovery transmissions in LTE networks with fractional frequency reuse,” Comput. Netw. **88**, 149–160 (2015).
[34] H. Liu, P. Xia, Y. Chen, *et al.*, “Interference graph-based dynamic frequency reuse in optical attocell networks,” Opt. Commun. **402**, 527–534 (2017).
[35] N. Titi, S. Haddad, A. Soukkou, F. Aknouche and H. E. Djema, "Power Allocation Optimization Using Water-Filling Technique for MIMO-NOMA-Based Visible Light Communication Systems," 2024 International Conference on Advances in Electrical and Communication Technologies (ICAECOT), Setif, Algeria, 2024, pp. 1-6, doi: 10.1109/ICAECOT62402.2024.10829012.